CSIRO PUBLISHING

Australian Journal of Physics

Volume 52, 1999

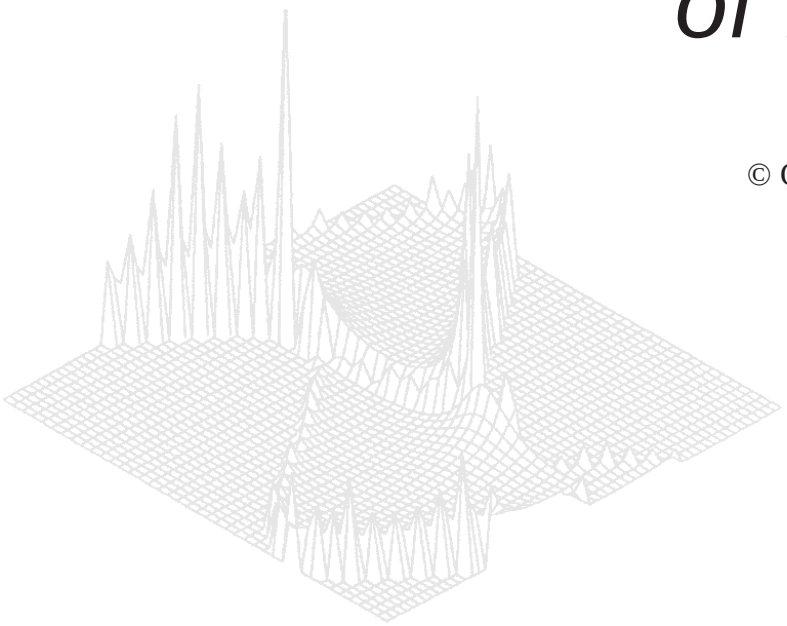

A journal for the publication of
original research in all branches of physics

www.publish.csiro.au/journals/ajp

All enquiries and manuscripts should be directed to
Australian Journal of Physics
CSIRO PUBLISHING
PO Box 1139 (150 Oxford St)
Collingwood Telephone: 61 3 9662 7626
Vic. 3066 Facsimile: 61 3 9662 7611
Australia Email: peter.robertson@publish.csiro.au

Published by **CSIRO** PUBLISHING
for CSIRO Australia and
the Australian Academy of Science

Aust. J. Phys., 1999, **52**, 563–78

Some Recent Developments in the Photoelectron Spectroscopy of Solids*

Robert Leckey

Department of Physics, La Trobe University,
Bundoora, Vic. 3083, Australia.

Abstract

A selective review of some recent achievements in the general area of the photoelectron spectroscopy of solids is presented emphasising full hemisphere data collection. The current state of development of both surface structure and electronic band structure determinations is illustrated with an emphasis on materials for which electron correlation effects are significant.

1. Introduction

As with most experimental procedures, the development of the technique of photoelectron spectroscopy has involved the consideration of ever more complex systems for which an increasing number of parameters can be determined. The movement towards a 'complete' photoemission experiment has been assisted by the increasing availability of synchrotron radiation sources and by increasing sophistication in the design of electron spectrometers. Whereas it was sufficient to obtain density of states information by means of an angle integrated experiment on a polycrystalline material in the early 1970*s*, a state of the art photoemission experiment may now involve circularly polarised light and an 'exotic' sample such as a multiple quantum well crystal, combined with a spin selective, angle resolved spectrometer.

This paper is an attempt to illustrate the capabilities of modern photoelectron spectroscopy for the determination of both surface structure and of the electronic band structure of crystalline materials by means of a few selected examples. The topics chosen inevitably have been influenced by the interests of the author as well as by the topic of the Fremantle workshop, i.e. the study of correlated systems.

2. Structural Information

X-ray photoelectron diffraction (XPD) has matured into a technique capable of answering rather detailed questions concerning the atomic structure of quite complex situations. Although the precision with which atomic locations can

* Refereed paper based on a contribution to the Australia–Germany Workshop on Electron Correlations held in Fremantle, Western Australia, on 1–6 October 1998.

 10.1071/PH98079 0004-9506/99/030563$05.00

routinely be determined is not so high as is the case with the most sophisticated LEED methods (Heinz 1988), XPD in both single photon energy–full hemisphere detection mode (Fadley 1993; Osterwalder *et al.* 1995), or in scanned photon energy mode (Dippel *et al.* 1992), has provided significant new structural information on many systems of fundamental and technical interest.

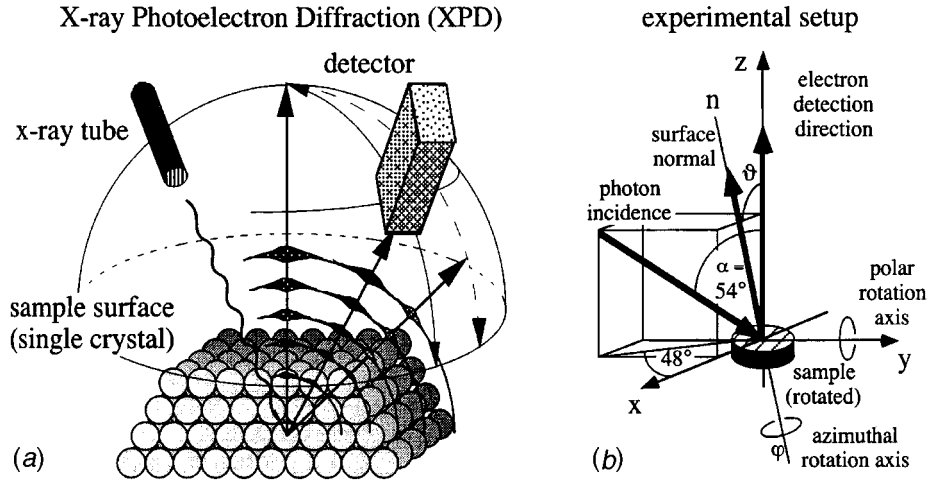

Fig. 1. The geometry for a full-hemisphere X-ray photoelectron diffraction experiment. [From Fasel (1996).]

The experimental geometry needed for fixed photon energy XPD is shown in Fig. 1. By rotating the sample in both azimuthal ϕ and polar θ senses, an intensity map generated by a selected core photoemission line may be collected which covers the entire emission hemisphere. Features resulting from the predominant forward scattering of medium energy electrons dominate such a map. These features illustrate crystallographic directions rather directly and are surrounded by weaker diffraction features, which carry information about inter-atomic distances. To extract the latter it has been necessary to calculate the intensity pattern to be expected based on an assumed atomic structure using a single or multiple scattering formalism (Rehr *et al.* 1986) followed by iterative adjustment to the originally assumed structural model to achieve the best fit to experiment. The availability of full hemisphere data, as opposed to individual polar or azimuthal scans, has improved the accuracy of this iterative procedure, whereas the availability of increased computing power has recently made it possible to automate the structural determination process. An example of the use of a so-called *R*-factor analysis (Fasel and Osterwalder 1995) is shown in Fig. 2 for the $c(2\times2)$-Na/Al (001) case. By examining not only the three structural models illustrated but also the possibility of the co-existence of domains involving both hollow and substitutional sites, the R-factor analysis results in a much improved agreement between simulated and experimentally measured intensity data whenever a 50/50 incoherent superposition of the latter two sites is postulated.

As a second example of the power of the XPD technique, Fig. 3 illustrates the result of an extended study into the adsorption geometry assumed by C_{60}

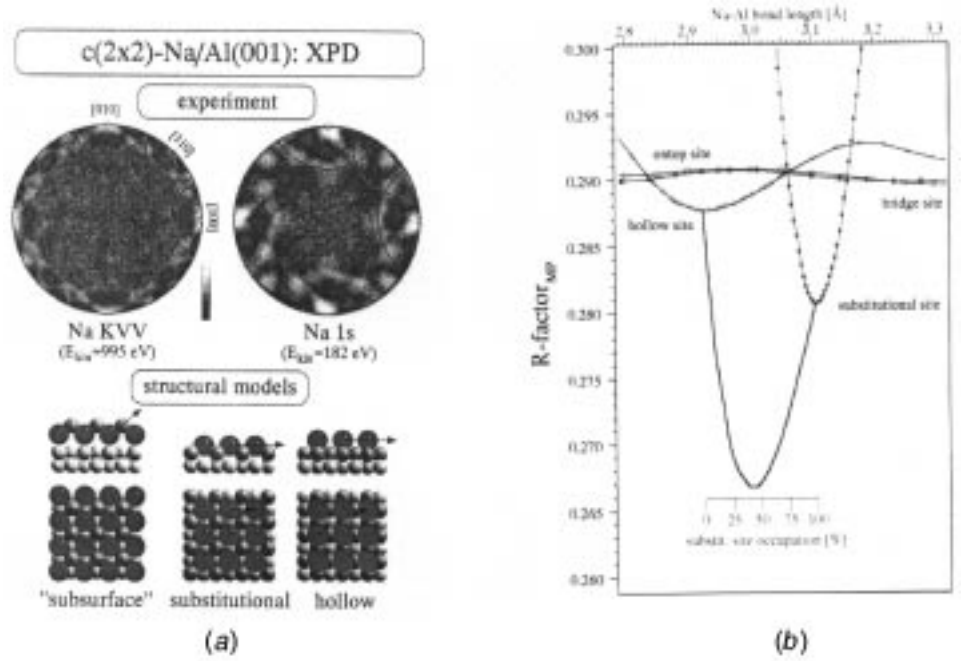

Fig. 2. (a) Three possible structural models for the system $c(2\times2)$-Na/Al(001) and representative XPD maps. (*b*) Results of an optimising *R*-factor analysis indicating that best agreement with experiment is achieved when a 50/50 mixture of hollow and substitutional site adsorptions is assumed. [From Fasel and Osterwalder (1995).]

molecules on selected crystalline surfaces. Here it has been determined, for example, that on Cu(111) a six-ring face of C_{60} is oriented facing the surface in two azimuthal orientations differing by 60°, whereas on Ni(001) adsorption takes place on a 6–6 bond aligned along the {010} surface directions. Further details may be found in Fasel and Osterwalder (1995).

An alternative procedure to extract structural information from XPD maps was proposed by Szoke (1986) and developed by Barton (1988) and by others (see e.g. Tonner *et al.* 1991). Reconstruction of single photon energy XPD maps via this holographic-like concept has proved to be dominated by artifacts introduced by the non-isotropic nature of photoelectron emission and by the large phase shifts typical of elastic scattering by medium energy electrons (as contrasted with X-ray scattering) (Denecke *et al.* 1995). More promising results have been obtained by combining a number of intensity maps collected over a wide range of photon energies (or electron momenta). The expectation is that interference based on pathlength differences between scattering centres will be invariant with photon energy unlike scattering phase shift effects. The concept behind one such approach is shown as Fig. 4*a*. In an investigation of the adsorption of Al on Si (111) (Wu *et al.* 1993), intensity data from the Al 2p core level were acquired at multiple emission angles and for many photon energies. Subtraction of a smooth background, partially due to varying monochromator efficiency, from each energy scan results in a (vector) function of momentum which can be Fourier transformed to provide three-dimensional real space information. The results are

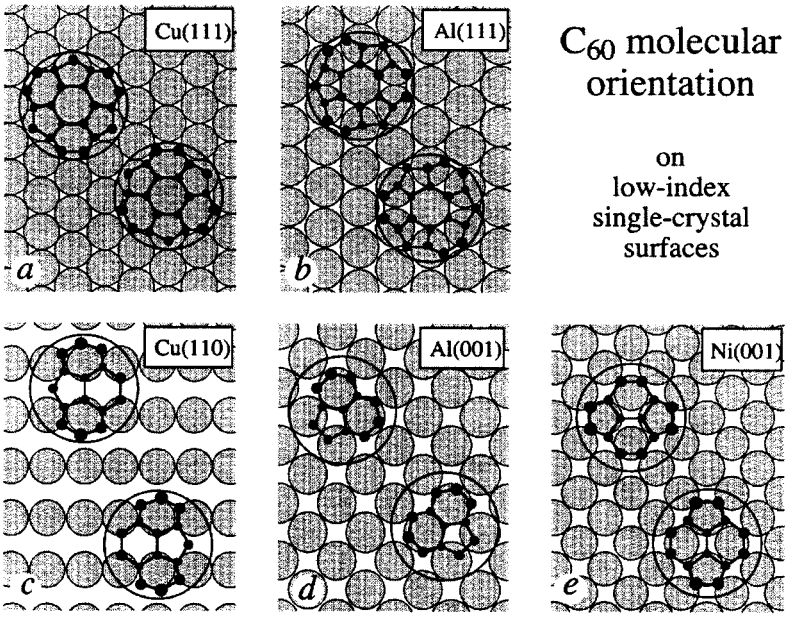

Fig. 3. Results of a detailed investigation into the adsorption geometry assumed by C_{60} on various low index crystal faces. [From Fasel and Osterwalder (1995).]

illustrated in Figs 4*b* and 4*c* in terms of horizontal and vertical slices, which confirm the geometry shown in Fig. 4*d*.

More recently, intensity oscillations in the branching ratio of the Bi 5d core level associated with diffraction effects and occurring as a function of photon energy have been used in conjunction with a holographic inversion procedure to establish the trimer structure of this atom on Si (111) (Roesler *et al.* 1997). The advantage of this method lies with the fact that by monitoring the intensity variations of both lines of a spin–orbit doublet and then taking the ratio of these intensities, instrumental and other slowly varying scattering effects mostly cancel out and the Fourier transformed data does not exhibit strong artifacts. The holographic method does not require surface modeling simulations but rather is a more direct structural technique than is the *R*-factor iterative XPD method. The positional accuracy for adsorbates such as Bi on Si is currently around 0·5 Å, however, which is significantly poorer than full-scale LEED determinations (Wan *et al.* 1991).

It may also be noted that the collection of full hemisphere intensity data in a low energy ion scattering spectroscopic (LEISS) experiment can also provide extremely surface sensitive structural information (Agostino *et al.* 1997).

3. Electronic Structure

(3a) Valence Band Structure

For many years, the most prominent use of angle resolved ultra-violet photoemisssion (ARUPS) has been the determination of the electronic band

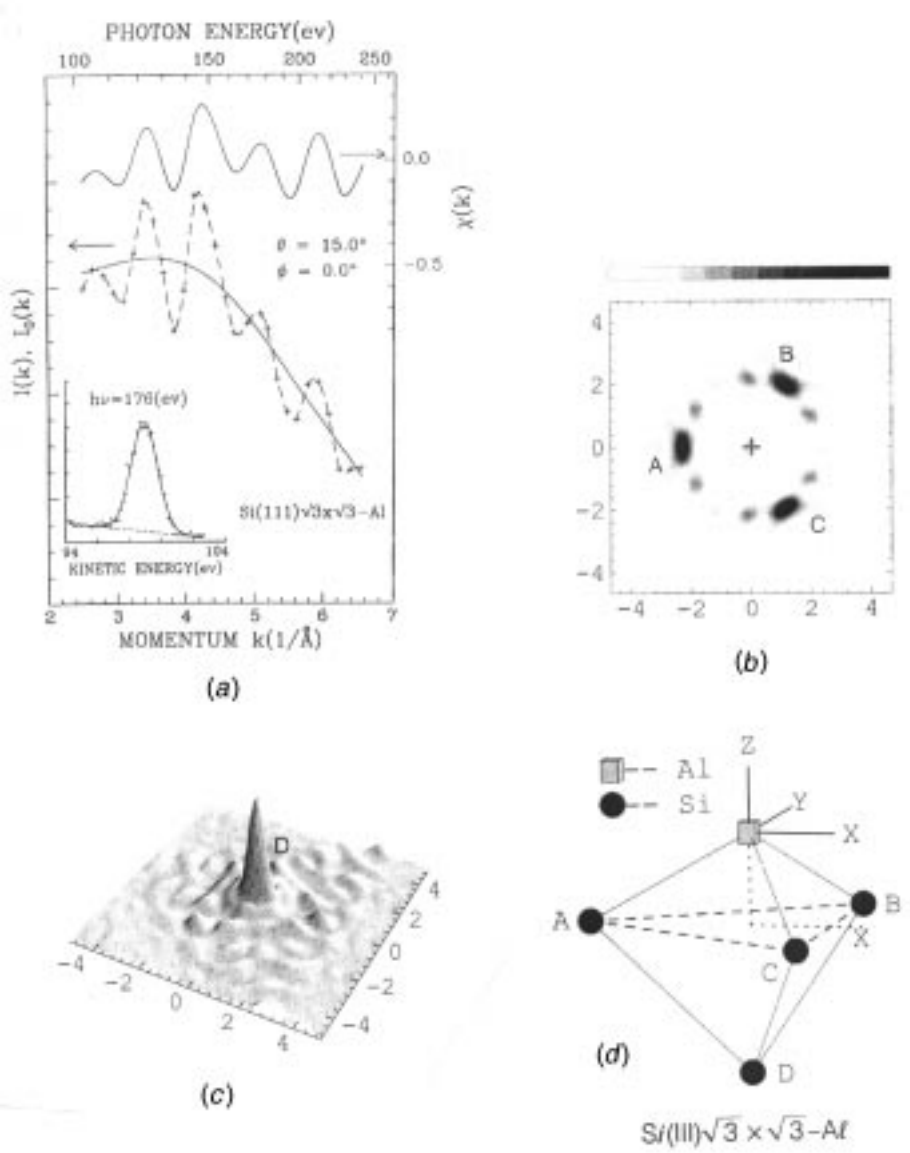

Fig. 4. (a) Representative intensity scan $I(k)$ at a polar angle of 15° of the Al 2p core level as a function of photon energy and an anisotropy function $\chi(k)$ obtained after background subtraction. (b) Holographically inverted map in the horizontal plane containing the three Si atoms shown in (d). (c) Similar horizontal cut for the plane containing the Si atom labelled D in (d). [From Wu *et al.* (1993).]

structure of metals and semiconductors. This has usually involved the collection of a set of energy distribution curves for normally emitted electrons covering a range of photon energies typically from 25 to 100 eV. The assumption is usually made that the final state of the electrons can be modeled sufficiently accurately by the free electron dispersion formula, $k = 0.511\sqrt{E}$, where k is in inverse Angstrom

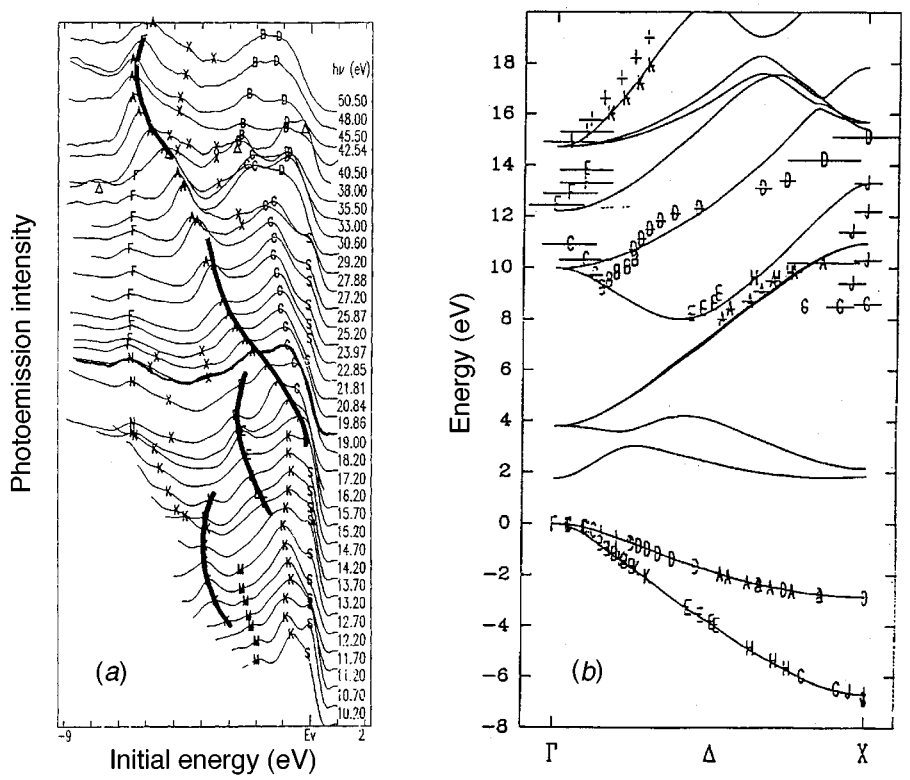

Fig. 5. (*a*) Set of energy distribution curves from GaAs (001) obtained with p-polarised light with energy as indicated. Peaks arising from transitions from bulk valence bands are indicated with letter symbols; those labeled S are surface states. (*b*) Excited state bands obtained from the data in (*a*) when the valence band states are assumed to be given precisely by an LMTO calculation. [From Zhang *et al.* (1993).]

units and the kinetic energy E is in eV. Justification for this assumption largely rests on the shortness of the mean-free-path for inelastic scattering by the electrons within the material and the consequent lifetime broadening of the real final states involved, together with the increasing multiplicity of free electron branches available as the kinetic energy increases. The need to use such an uncertain intermediate state for the evaluation of initial (valence) band states nevertheless remains a rather undesirable aspect of this technique. The use of theoretical bands is not an option due to the lack of excited, as opposed to ground state calculations extending to sufficiently high energies. The suitability of calculated ground state bands within 20 eV of the valence band maximum in GaAs may be judged from Fig. 5. In this experiment (Zhang *et al.* 1993), the calculated valence bands were taken as accurate and the normal data processing method inverted to illustrate the apparent position of the final states involved. It is clear from Fig. 5 that a low energy approach utilising calculated final state bands is unlikely to succeed as a method for evaluating the valence band states. One conclusion that might be reached is that the current state of band structure calculations is such that, for many simple materials, a theoretical approach is more likely

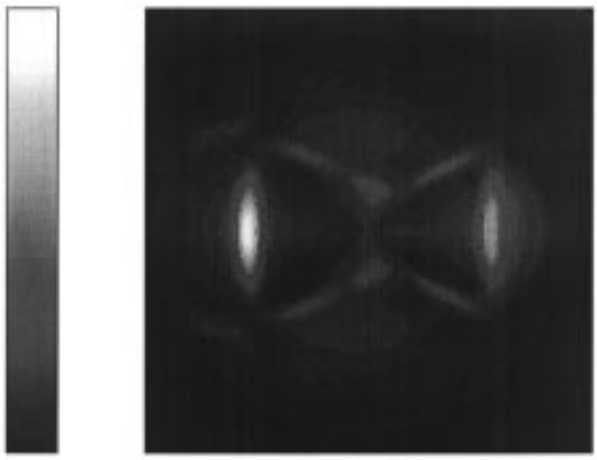

Fig. 6. Fermi surface map from Cu (110) using 24·0 eV p-polarised photons showing the 'dog' s bone' orbit. [From Stampfl *et al.* (1995).]

to provide accurate eigen-energies than is the ARUPS method. Consequently, experimental effort should be directed towards the determination of the band structure of those classes of materials for which the theory remains intractable. Most alloys and many oxides fall into such a category.

(3b) Fermi Surface Topology

In recent years, attention has been concentrated on the ability of the photoemission method to determine the topology of the Fermi surface of metals and alloys. Although remaining dependent on the free electron final state assumption, the real advantage of this method over the standard de Haas–van Alphen technique (Landoldt–Bornstein 1984) is that it is viable at elevated temperatures and can investigate substitutionally disordered alloys. These advantages compensate for the lesser precision of the photoemission method at the current stage of its development.

Fermi surface maps may be obtained from (a) a full hemisphere intensity map with the spectrometer tuned to the Fermi energy as initial state (Con Foo *et al.* 1996; Aebi *et al.* 1994*a*) or (b) from a constant initial state (CIS) procedure. The former provides a projection of an approximately spherical slice through the Fermi surface as illustrated in Fig. 6. Here the original $I(\theta, \phi)$ data have been transformed into a k_x, k_y map using the relations $\theta = \arcsin[(k_x{}^2+k_y{}^2)/|k^2|]$ and $\phi = \arctan |k_x/k_y|$. Such maps are particularly useful at illustrating the symmetry of the Fermi surface directly (see Fig. 6).

In method (b), the photon energy and the kinetic energy of detection are altered in synchronism and $I(\theta)$ data collected. Assuming free electron final states, this method shows high intensity at those k-space locations where the free electron sphere associated with each kinetic energy and the initial state Fermi surface intersects, as illustrated in Fig. 7. This procedure provides a linear slice through the Fermi surface and provides k-space dimensions rather directly.

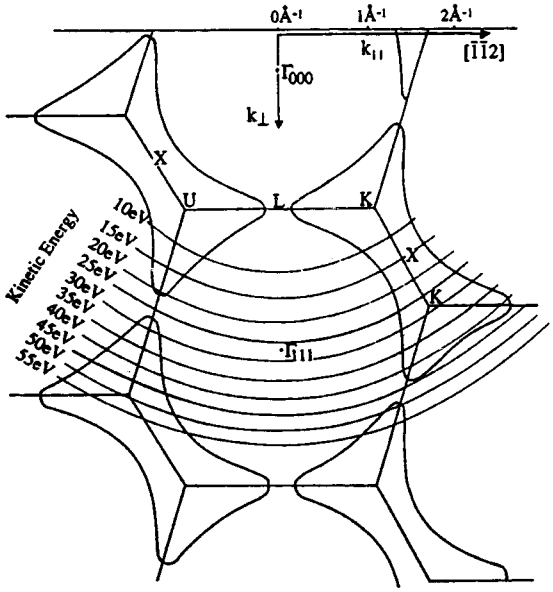

Fig. 7. Section through the Fermi surface of Cu in the [111] plane together with circles representing free-electron-like excited states covering a range of kinetic energies. High intensity is expected in a CIS experiment where initial (Fermi energy) and final states intersect. [From Stampfl *et al.* (1995).]

We have used the CIS procedure to investigate the dimensions of the Fermi surface of the alloy Cu_3Au on both substitutionally disordered and ordered phases: typical results are shown in Fig. 8 (Con Foo *et al.* 1996). Cu_3Au undergoes a first order phase transition from a face-centred cubic disordered structure to an ordered LI_2 structure at 390°C. The Brillouin zone of the ordered structure is half that of the disordered structure and it is therefore of interest to compare the 'neck' and 'belly' radii of the two Fermi surfaces. Con Foo *et al.* found that the neck radius was unchanged by the phase transition, but that the belly radius increased by as much as 30% in the disordered phase.

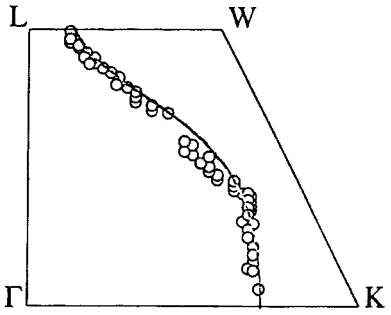

Fig. 8. Experimental Fermi surface cross section of Cu_3Au from the (111){110} plane as determined by CIS photoemission. The solid line is a calculated section based on a simple rigid band model. [From Con Foo *et al.* (1996).]

(3c) Fermi Surface of the High T_c Superconductor Bi_{2212}

When applied to the high temperature superconductor Bi_{2212}, method (a) has been used (Aebi *et al.* 1994*b*) to demonstrate the fact that optimally doped material possesses a large Fermi surface centred on π, π. As well as the main Fermi surface profile, clearly shown in Fig. 9 are weak structures that have become known as shadow bands. Two explanations for these shadow bands, which take the form of a $c(2\times2)$ superstructure, have been proposed. Aebi *et al.* suggested that their origin may be explained by invoking the co-existence of some short-range anti-ferromagnetic order in room temperature Bi_{2212}. Although it would be surprising if such structure co-existed in the superconducting state, it is, however, the natural structure for insulating, under-doped material. The alternative explanation arises due to the so-called 5×1 structural superstructure that is known to modulate atomic positions along the *b*-crystal direction (Osterwalder *et al.* 1995). In an attempt to distinguish these possibilities, Schwaller (1997) has performed a controlled doping experiment on this compound. He found that continued exposure to intense UV light has the effect of transforming an optimally doped sample to a progressively under-doped condition. Since the under-doped compound is known to be anti-ferromagnetically ordered, it would be expected that the shadow band intensity would increase relative to the large Fermi surface intensity as the UV irradiation continued. Since this was not observed, the structural 5×1 explanation would appear to be favoured.

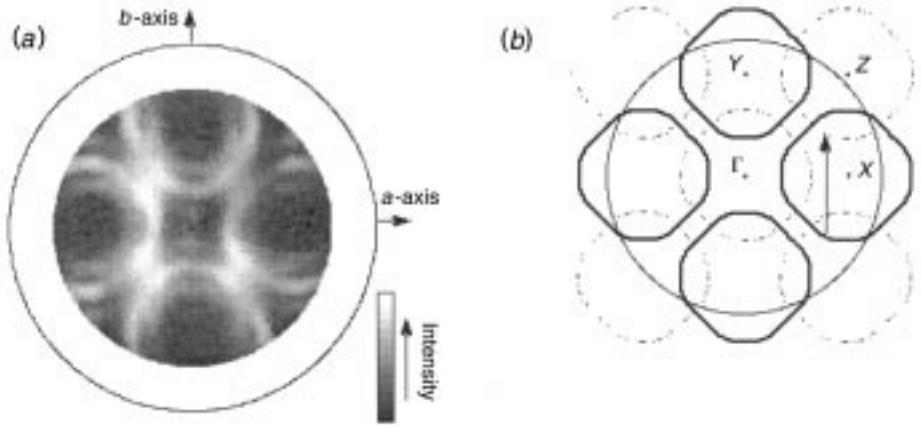

Fig. 9. (*a*) Fermi surface map from Bi_{2212} taken with unpolarised 21·21 eV photons showing (*b*) the large Fermi surface centred at Γ and associated shadow bands. [From Aebi *et al.* (1994*b*).]

(3d) Temperature and k-dependent Exchange Splitting in Ni

The electronic structure of the strong ferromagnet Ni has been investigated by many techniques over very many years, but there is as yet no established understanding of the high temperature behaviour of this material. A valuable review of the situation in 1993 was provided by Donath (1994), which includes a detailed discussion of the extent to which photoemission and inverse photoemission (including spin polarised data) has illuminated our understanding of behaviour

of the magnetic bands as a function of temperature. A significant body of information now exists which indicates that the exchange splitting in Ni is both temperature and k-dependent as discussed below. The question of whether short-range order exists above the Curie temperature remains controversial. In this section, a brief discussion of recent photoemission experiments on this topic will be presented.

From a theoretical perspective, a simple Stoner–Wohlfarth mean field model (Wohlfarth 1953) predicts the collapse of exchange splitting above T_c implying the disappearance of local moments. Fluctuating band models (Capellmann 1979; Korenmann and Prange 1980) have also been developed which allow for k-dependent exchange splittings and persisting moments above T_c, as have a number of variants which may be collectively be called disordered local moment theories (Hubbard 1981; Pindor *et al.* 1983). A many body approach based on a Hubbard model (Nolting *et al.* 1989) has been successful in predicting a reasonable value for T_c (unlike one-electron theories that overestimate T_c considerably). This approach has provided a useful quasi-particle band structure for elevated temperatures, which may usefully be compared with photoemission data and which predicts a k-dependent exchange splitting for quasi-particle d-like states close to the Fermi energy and a vanishing splitting as T_c is approached.

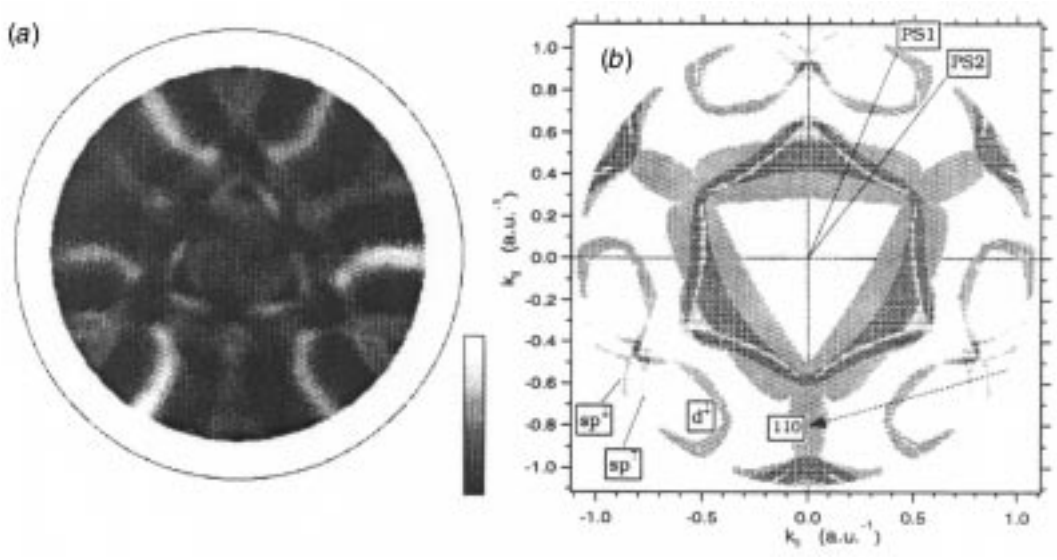

Fig. 10. (*a*) Fermi surface map from Ni(111) at room temperature using $21 \cdot 21$ eV photons. The data have been contrast enhanced and are shown in a stereographic projection. (*b*) Result of an LKKR calculation including spin assignments of selected states. [From Kreutz (1997).]

Neutron scattering experiments (Shirane 1984) and recent resonant photoemission data (Sinkovic et al. 1997) point to the existence of local moments above T_c, whereas recent ARUPS (Cai *et al.* 1997) and Fermi mapping data (Kreutz 1997) demonstrate Stoner-like collapsing behaviour for at least some bands. From an experimental perspective one can investigate three types of states: magnetic surface states, s–p-like states and d-like states close to E_f. Early spin-integrated

ARUPS investigations displaying energy distribution curves found it difficult to separate the spin-split bands in Ni due to the relatively small energy difference involved (<0·3 eV). Aebi *et al.* (1994*a*) however, have pointed out that pairs of spin-split bands at the Fermi energy are more readily distinguished in an ARUPS experiment by their k-space locations (essentially the polar angle of electron emission) than by their energy differences. While it is still necessary for a non spin-resolved experiment to rely on theory as a guide in identifying individual spin-split bands, this work has demonstrated that structures visible in a Fermi surface map can reasonably be associated unambiguously with particular states. Fig. 10 shows an enhanced Fermi surface map from Ni(111) taken with 21·21 eV photons compared with the result of a calculation which used LKKR initial states and free electron final states. This same work has also tracked the variation in the exchange splitting of the s–p bands at E_f in Ni(111) as a function of temperature and has found clear evidence of Stoner-like collapsing bands as shown in Fig. 11.

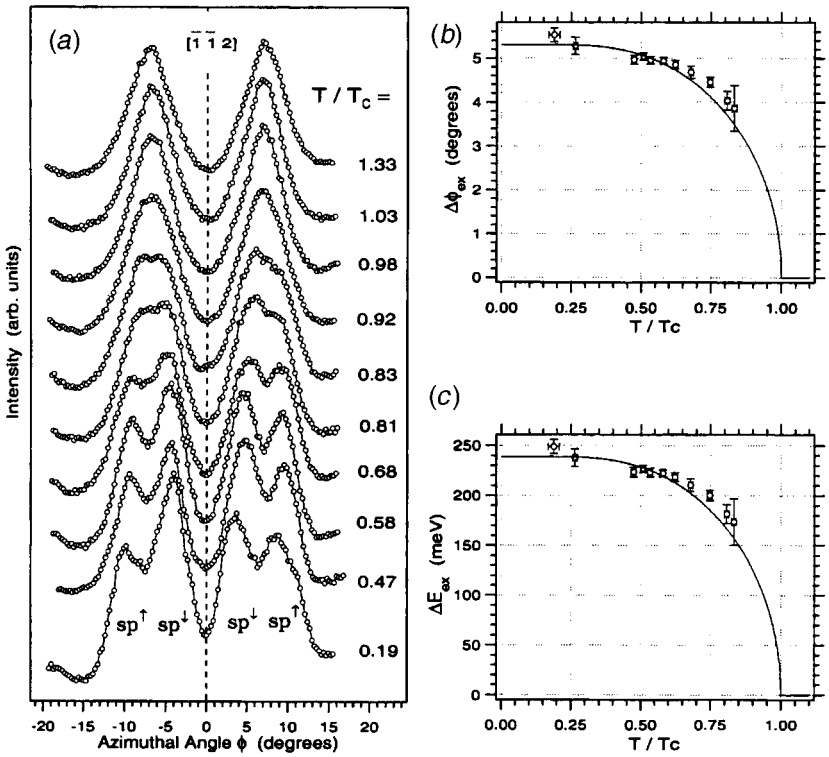

Fig. 11. (*a*) Angular profile of s–p bands at the Fermi energy in the vicinity of the [−1−1−2] direction in Ni (111) at a polar emission angle 78° as a function of temperature. Angular (*b*) and energy (*c*) exchange splittings as determined by peak fitting the data in (*a*) as a function of reduced temperature. [From Kreutz (1997).]

Cai *et al.* (1997) have recently revisited a study of the magnetic surface states on Ni(100) along the ΓX and ΓM directions previously investigated by Plummer and Eberhardt (1979). As with other ARUPS investigations without

spin detection, this study had to infer rather than directly observe individual spin bands. Nevertheless, the evidence pointed towards a non-vanishing exchange splitting above T_c as inferred from a line-shape analysis.

Direct evidence for the retention of dipole moments above T_c has recently been provided by a resonant photoemission study that used circularly polarised photons and spin detection of the electrons. Light of known helicity produces a spin polarised $2p_{3/2}$ or $2p_{1/2}$ core hole, following which subsequent Auger decay produces spin polarised electrons allowing the degree of polarisation of both singlet and triplet valence band excitations to be determined. The discussion in this paper is largely in terms of angular momentum rather than in the usual language of itinerant band electrons, but as shown in Fig. 12, the results clearly demonstrate the presence of local moments of mostly triplet nature close to the Fermi energy which remain above T_c.

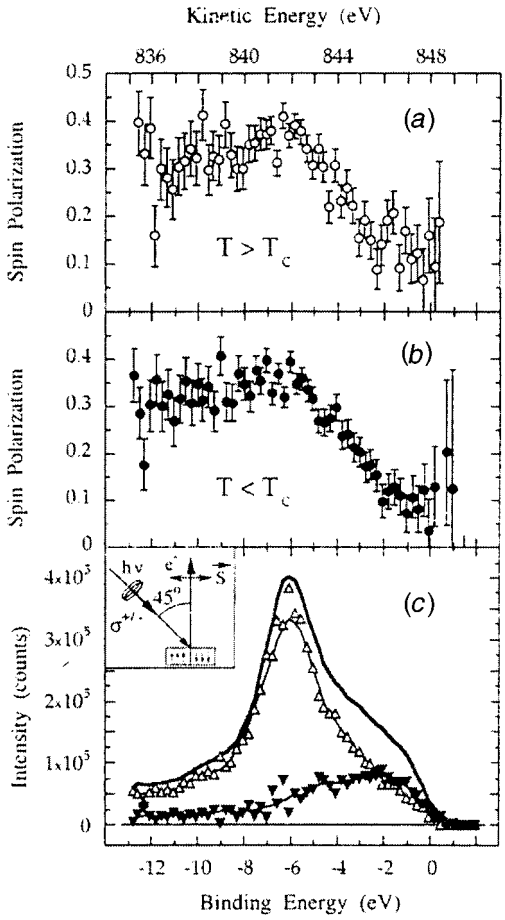

Fig. 12. Spin-resolved circularly-polarised $2p_{3/2}$ resonant valence band emission from Ni(001): (*a*) spin integrated spectrum (solid line) with singlet (triangles) and triplet (inverted triangles) contributions; fractional spin polarisation below (*b*) and above (*c*) the Curie temperature. [From Sinkovic *et al.* (1997).]

We have recently used the 'amplification' feature of CIS spectroscopy to further investigate Ni d-band behaviour with temperature (Stampfl *et al.* 1999). Due to the steep gradient of final state bands well above E_f, spin states separated to a

small degree in momentum are expected to give rise to well separated intensity peaks in a CIS spectrum as illustrated in Fig. 13*a*. The temperature dependence of two such peaks, which we have assigned to the Δ_5 minority and majority bands in Ni(001), clearly indicates non-collapsing behaviour above T_c (see Fig. 13*b*). It is, however, possible that some unexpected structure in the final states involved in this result may negate this preliminary interpretation.

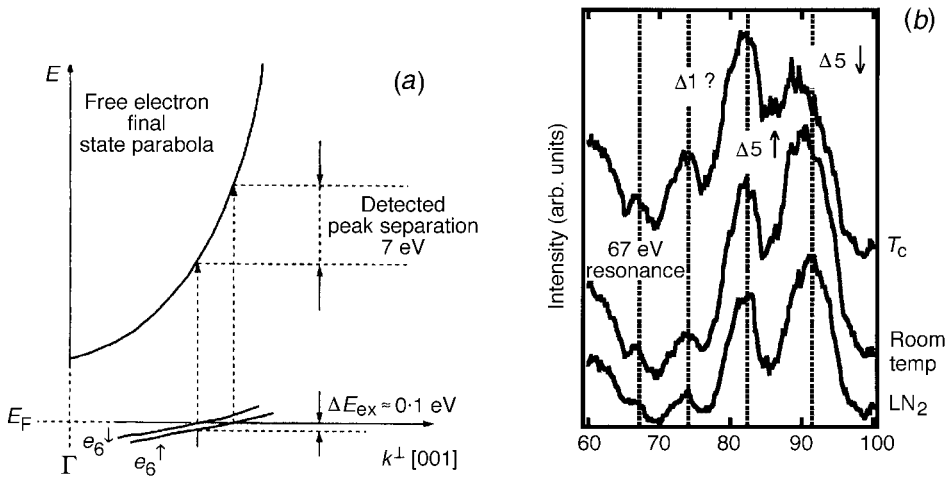

Fig. 13. (*a*) In a constant initial state experiment two states narrowly separated in energy and momentum may be observed widely separated in kinetic energy if the final state dispersion is large. (*b*) Constant initial state spectra covering the photon energy range 60–100 eV from Ni(001) [111]. The emission geometry has been selected to bracket the D_5 bands, the exchange splitting of which is seen to narrow but not to disappear at the Curie temperature as shown. [From Stampfl *et al.* (1999).]

We are therefore left with evidence from a wide variety of electron spectroscopic techniques which remains somewhat confusing but which will need to be included in any complete explanation of the high temperature behaviour of this intriguing metal.

(3e) Thin Film Magnetism

To illustrate further the capability of ARUPS to solve technologically interesting problems, mention can be made of two studies involving atomically thin layers of a magnetic material in conjunction with a non-magnetic one.

Mankey *et al.* (1997) have shown that a monolayer of Ni grown epitaxially on Cu(001) exhibits a bulk Fermi surface—see Fig. 14. The explanation given for this rather unexpected result is that the Ni sp-$d_z{}^2$ hybrid band is partially filled at E_f, facilitating hybridisation with the Cu s–p band.

Giant magnetoresistance multilayers are of significant interest in the data recording industry. The existence of an oscillation in the interlayer magnetic coupling of Fe/Cr (001) multilayers with period of 1·8 nm has been known for some time and has been thought to be determined by an extremal spanning vector of the Fermi surface of the non-magnetic spacer material. Possible nesting vectors, which have been suggested in the past, include those labeled a, b and c

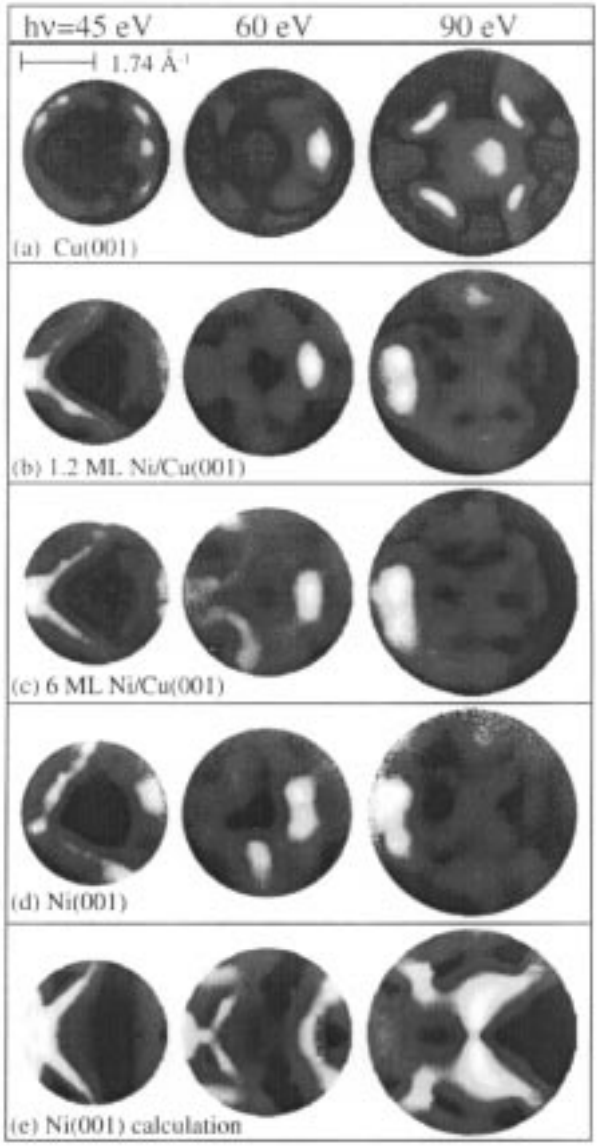

Fig. 14. Angular distributions of photoelectrons originating at the Fermi energy for three photon energies: (*a*) Cu (001), (*b*) 1·2 monolayer (ML) thickness of Ni on Cu (001), (*c*) 6 ML film, (*d*) Ni (001) and (*e*) theoretical map for Ni (001). [From Mankey *et al.* (1997).]

in Fig. 15*a*. The intensity variation of quantum well states close to the Fermi energy at k-parallel locations corresponding to each of these nesting vectors has been observed by Li *et al.* (1997). This work has established that the vector associated with the 'lens' (labelled a in Fig. 15*a*) shows a clear variation of 1·7 nm period with Cr thickness. No comparable periodicities were observed at k-parallel locations associated with the other candidate nesting vectors.

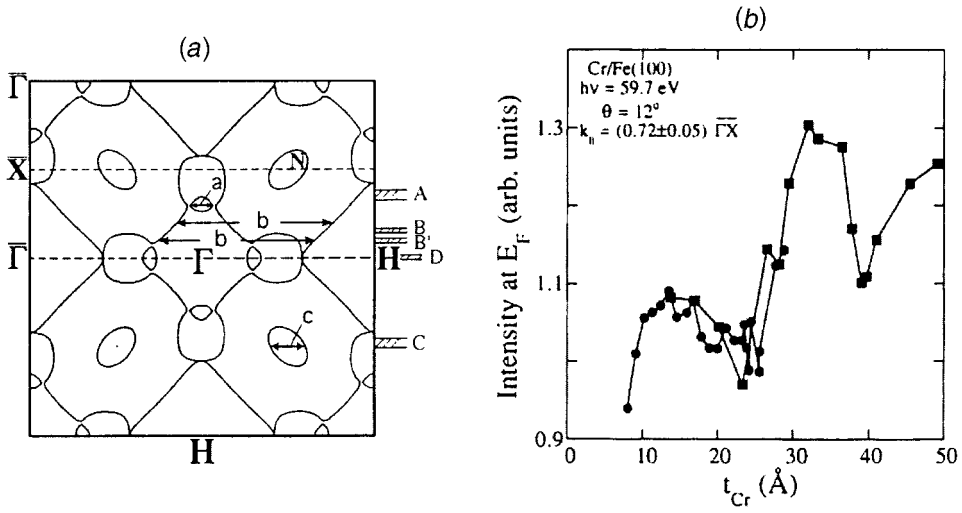

Fig. 15. (*a*) Calculated Fermi surface of Cr [11]. Spanning vectors possibly involved in long period magnetoresistive oscillations in Fe/Cr multilayers are identified by letter symbols. (*b*) Intensity variation of a quantum well state observed when the parallel component of momentum along ΓX is set to correspond with the lens-shaped structure labelled 'a' above. [From Li *et al.* (1997).]

4. Summary

Selected examples of recent photoemission data have been presented in an attempt to illustrate some of the capabilities of the technique. The author is acutely aware that this mini-review does not do justice to the topic and that many exciting developments have been omitted. In particular, much development is being undertaken at third generation synchrotron radiation sources where intrinsically high emittance enables significant advances in spectro-microscopy of various types. Similarly, magnetic dichroism studies have not been discussed here primarily due to space limitations. Angle resolved photoemission may have matured over recent years, but there are no signs that it will cease to evolve into an ever more powerful surface science technique.

Acknowledgments

I am most grateful to my colleagues at La Trobe University, particularly John Riley and Anton Stampfl, and to Philipp Aebi and Roman Fasel of the Institute of Physics, Université de Fribourg, for many valuable and informative discussions. Photoemission research at La Trobe is supported by the Australian Research Council.

References

Aebi, P., Osterwalder, J., Fasel, R., Naumovic, D., and Schlapbach, L. (1994*a*). *Surf. Sci.* **307–9**, 917.

Aebi, P., Osterwalder, J., Schwaller, P., Schlapbach, L., Shimoda, M., Mochiku, T., and Kadowaki, K. (1994*b*). *Phys. Rev. Lett.* **72**, 2757.

Agostino, R. G., Aebi, P., Osterwalder, J., Hayoz, J., and Schlapbach, L. (1997). *Surf. Sci.* **384**, 36.

Barton, J. J. (1988). *Phys. Rev. Lett.* **61**, 1356.
Cai, Y. Q., Bradshaw, A. M., Stampfl, A. J. P., Tkatchenko, S., Riley, J. D., and Leckey, R. C. G. (1997). *Surf. Sci.* **377–9**, 470.
Capellmann, H. (1979). *Z. Phys.* B **34**, 29.
Con Foo, J. A., Tkatchenko, T., Stampfl, A. J. P., Ziegler, A., Mattern, B., Hollering, M., Ley, L., Riley, J. D., and Leckey, R. C. G. (1996). *Surf. Interface Anal.* **24**, 535.
Denecke, R., Eckstein, R., Ley, L., Bocquet, A. E., Riley, J. D., and Leckey, R. C. G. (1995). *Surf. Sci.* **331–3**, 1085.
Dippel, R., Woodruff, D. P., Hu, X-M., Asensio, M. C., Robinson, A. W., Schindler, K.-M., Weiss, K. U., Gardner, P., and Bradshaw, A. M. (1992). *Phys. Rev. Lett.* **68**, 1543.
Donath, M. (1994). *Surf. Sci. Rep.* **20**, 251.
Fadley, C. S. (1993). *Surf. Sci. Rep.* **19**, 231.
Fasel, R. (1996). PhD thesis, University of Fribourg, Switzerland.
Fasel, R., and Osterwalder, J. (1995). *Surf. Rev. & Lett.* **2**, 359.
Heinz, K. (1988). *Prog. Surf. Sci.* **27**, 239.
Hubbard, J. (1981). *Phys. Rev.* B **23**, 5974.
Korenmann, V., and Prange, R. E. (1980). *Phys. Rev. Lett.* **44**, 291.
Kreutz, T. J. (1997). PhD thesis, University of Zurich, Switzerland.
Landolt-Bornstein (1984). 'Electron States and Fermi Surfaces of Elements', Vol. 13c (Springer: Berlin).
Li, D., Pearson, J., Bader, S. D., Vescovo, E., Huang, D.-J., and Johnson, P. D. (1997). *Phys. Rev. Lett.* **78**, 1154.
Mankey, G. J., Subramanian, K., Stockbauer, R. L., and Kurtz, R. L. (1997). *Phys. Rev. Lett.* **78**, 1146.
Nolting, W., Borgiel, W., Dose, V., and Fauster, Th. (1989). *Phys. Rev.* B **40**, 5015.
Osterwalder, J., Aebi, P., Fasel, R., Naumovic, D., Schwaller, P., Kreutz, T. J., Schlapbach, L., Abukawa, T., and Kono, S. (1995). *Surf. Sci.* **331–3**, 1002.
Pindor, A. J., Staunton, J., Stocks, G. M., and Winter, H. (1983). *J. Phys.* F **13**, 979.
Plummer, E. W., and Eberhardt, W. (1979). *Phys. Rev.* B **20**, 1444.
Rehr, J. J., Albers, R. C., Natoli, C. R., and Stern, E. A. (1986). *Phys. Rev.* B **34**, 778.
Roesler, J. M., Sieger, M. T., Miller, T., and Chiang, T.-C. (1997). *Surf. Sci.* **380**, L485.
Schwaller, P. (1997). PhD thesis, University of Zurich, Switzerland.
Shirane, G. (1984). *J. Appl. Phys.* **55**, 1887.
Sinkovic, B., Tjeng, L. H., Brookes, N. B., Goedkoop, J. B., Hesper, R., Pelligrin, E., de Groot, F. M. F., Altieri, S., Hulbert, S. L., Shekel, E., and Sawatzky, G. A. (1997). *Phys. Rev. Lett.* **79**, 3510.
Stampfl, A. J. P., Con Foo, J. A., Leckey, R. C. G., Riley, J. D., Denecke, R., and Ley, L. (1995). *Surf. Sci.* **331–3**, 1272.
Stampfl, A. P. J., Riley, J. D., and Leckey, R. C. G. (1999). to be published.
Szoke, A. (1986). *In* 'Short Wavelength Coherent Radiation: Generation and Applications', AIP Conf. Proc. No. 147 (Eds D. T. Attwood and J. Boker), p. 361 (AIP: New York).
Tonner, B. P., Han, Z.-L., Harp, G. R., and Saldin, D. K. (1991). *Phys. Rev.* B **43**, 14423.
Wan, K. G., Guo, T., Ford, W. K., and Hermanson, J. C. (1991). *Phys. Rev.* B **44**, 3471.
Wohlfarth, E. P. (1953). *Rev. Mod. Phys.* **25**, 211.
Wu, H., Lapeyre, G. J., Huang, H., and Tong, S. Y. (1993). *Phys. Rev. Lett.* **71**, 251.
Zhang, X. D., Riley, J. D., Leckey, R. C. G., and Ley, L. (1993). *Phys. Rev.* B **48**, 17077.

Manuscript received 1 October 1998, accepted 22 February 1999